doi:10.1017/S1431927615013240

Fast *k*-Space Mapping of Electronic Bands Using Time-of-Flight Based Cathode-Lens Microspectroscopy.

Gerd Schönhense

Institut für Physik, Johannes Gutenberg-Universität, 55128 Mainz, Germany

Owing to the translational symmetry of crystalline solids, the electronic structure can be reduced to the first Brillouin zone, which contains the full information on all electronic bands. Experimental band mapping via angle-resolved photoelectron spectroscopy (ARPES) is characterized by excellent resolution (few meV and 0.2°) and has gained tremendous importance for the analysis of complex ***k***-space topologies and 3D spin textures [1]. The common ARPES-approach employs hemispherical energy analyzers. After half a century of development these analyzers have nowadays reached a high level of sophistication, but also their principal limits. Inherently, these analyzers are limited in the accepted solid angle interval to several degrees and one azimuthal plane, depending on the desired angular resolution. Along with an increasing demand for energy and angular resolution, data-acquisition speed has become an issue, in particular for reactive surfaces and –dramatically– when it comes to spin-resolved detection. The low performance of present (single-channel) spin detectors is prohibitive for many experiments.

This contribution addresses an alternative way of ***k***-resolved photoelectron spectroscopy (spin-integral and spin-resolved) aiming at a higher degree of parallelization in data acquisition. The novel concepts will be most important for time-resolved studies of transient states and spin-resolved spectroscopy. The underlying idea is rather simple and makes use of a basic concept of microscopy: In each imaging optical system the reciprocal image represents the distribution of the transversal momentum components. In mathematical language we can term it the Fourier image, providing the distribution of "spatial frequencies" (being nothing else than the momentum pattern). Owing to $\boldsymbol{k}_{\parallel}$-conservation in the photoemission process, the reciprocal image formed by the objective lens of a photoemission microscope directly yields the surface-projected band structure inside the crystal. This image occurs in the back focal plane of the cathode lens [2].

In momentum microscopy this Fourier pattern is imaged with ultimate ***k***-resolution. The intriguing advantage is that this method gives access to the $\boldsymbol{k}_{\parallel}$–distribution of a large fraction of the half-space above the solid. Given sufficiently high photon energy, the half space corresponds to a large momentum range exceeding the first Brillouin zone. Fig. 1 shows calculated trajectories for photoelectrons with starting energies of 5 keV (45° cone) and 100 eV (full 90° cone). In the high-energy case, which is typical for the bulk-sensitive method of hard X-ray photoemission (HAXPES), a momentum disc of 25 $Å^{-1}$ radius is observed simultaneously. Such a large solid angle at such a high energy is inaccessible using conventional HAXPES spectrometers. In the low-energy example of 100 eV the diameter reduces to 5 $Å^{-1}$, which still comprises several Brillouin zones. The objective lens of a momentum microscope is optimized for best resolution in ***k***-space. A benchmark has been set by a new instrument at the Max Planck Institute for Microstructure Physics in Halle (Germany), where a momentum resolution of 5×10^{-3} $Å^{-1}$ (along with an energy resolution of 12 meV) has been reached [3].

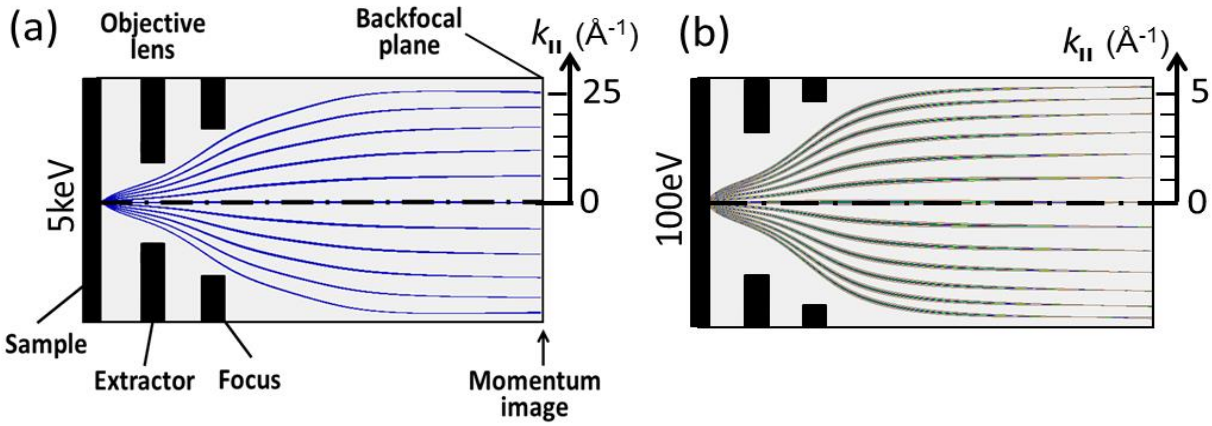

Figure 1. Trajectories in a cathode lens for photoelectrons with starting energies of 5 keV (a) and 100 eV (b). For (a) a cone with half angle of 45° and for (b) electrons starting into the full half space have been simulated.

There are two different ways of energy discrimination in momentum microscopes. Implementation of an imaging dispersive analyzer allows displaying of the $\boldsymbol{k}_{\parallel}$-distribution at a selected energy. This method was pioneered by J. Kirschner's group at MPI Halle [e.g. 4,5], employing an aberration-corrected tandem hemispherical analyzer. An imaging spin filter yields unprecedented spin-resolved acquisition speed. A spin-polarizing mirror for parallel imaging microscopes was first described in [6].

Impressive $\boldsymbol{k}$-patterns have been measured, e.g., for Cu [4,5]. A typical result for the Cu(001) surface is shown in Figure 2. Comparison with a calcuation (by J. Henk et al., Halle) reveals that a self-energy correction with parameters Σ_d = -0.8eV and Σ_{sp}=+0.3eV yields best agreement between experiment and theory (for details, see [5]). In principle, $\boldsymbol{k}_{\parallel}$-images of the full half space at the selected energy like those in Figure 2 can be observed on the fluorescence screen of the momentum microscope with the bare eye in real time (provided the photon flux is sufficiently high). 2D $\boldsymbol{k}_{\parallel}$–distributions at different energies are acquired sequentially.

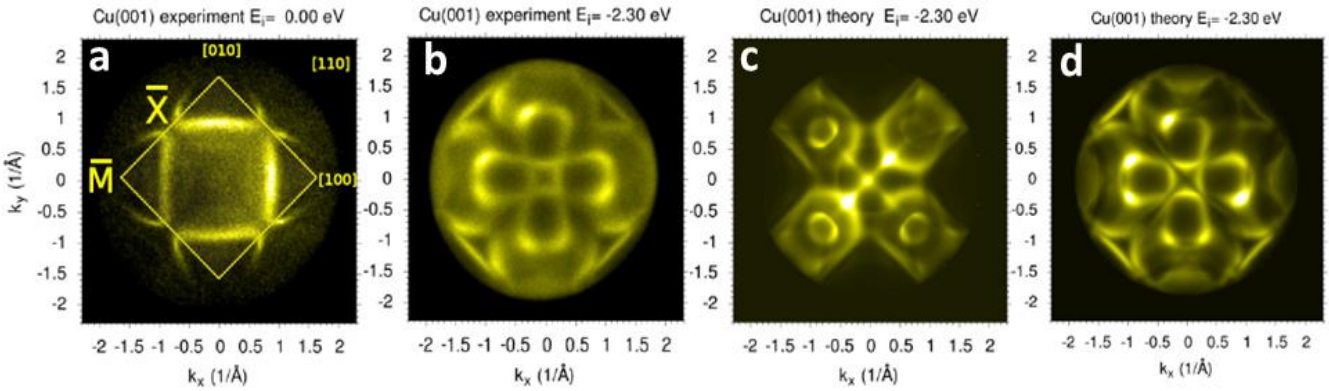

Figure 2. Momentum microscopy images of Cu (001) at the Fermi energy (a) and at a binding energy of 2.3 eV (b) in comparison with a calculation without (c) and with self-energy correction (d); (from [5]).

https://doi.org/10.1017/S1431927615013240 Published online by Cambridge University Press

Going further in parallelization, the Mainz group in cooperation with the Max Planck Institute in Halle are developing the time-of-flight momentum microscope, a 3D-method for ***k***-space mapping with utmost efficiency. It implements an imaging ToF spectrometer instead of the dispersive (i.e. bandpass-type) spectrometer. This approach adopts the concept of ToF-PEEM [7,8]; the heart of the experiment is a 3D (k_x,k_y,t)-resolving image detector (delay-line detector) [9,10] with 150 ps time resolution and 10 Mcps maximum count rate. The ToF way of energy discrimination bears the advantage that many energy surfaces are acquired simultaneously. It requires pulsed photon sources, like synchrotron radiation, lasers or high-harmonic sources.

Figure 3 shows a schematic cross section of the ToF ***k***-microscope with trajectories for 100 eV starting energy and a drift energy of 30 eV in the ToF section. The initial part up to the first *k*-image in the back focal plane (BFP) of the objective lens is identical to Figure 1. A size-selectable and adjustable field aperture is located in the first Gaussian image plane. It defines the source spot on the sample surface in a range of 25 to 150 μm, independent on the focusing quality of the photon source. In a momentum microscope the ***k***-image is magnified onto the image detector. In this case the selected field of view acts in the same way as the usual contrast aperture (placed in a reciprocal image plane) of a conventional real-space photoelectron microscope (PEEM). For sufficiently high photon flux density on the sample, a field of view down to the few-micrometer range can be selected in the first Gaussian plane, at the expense of a smaller accessible momentum disc.

A zoom lens transforms the electron beam to the desired drift energy in the imaging time-of-flight spectrometer. Photoelectron momentum maps and spectra are taken simultaneously in an energy interval of several eV width, limited by the chromatic aberration of the objective lens. The time resolution of the delay-line detector of 150 ps yields an energy dispersion of $\Delta E/meV = 0.255\ (E_d/eV)^{3/2}$ according to [11]. For the given length of the drift section (900 mm) drift energies between E_d = 40 eV and 4 eV thus lead to theoretical energy resolutions of ΔE = 40 meV down to 2 meV, respectively. The delay-line detector has an active area of 40 mm dia. and a spatial resolution of 50 μm, resolving 800 points along the image diagonal. The maximum integral count rate is 8 Mcps.

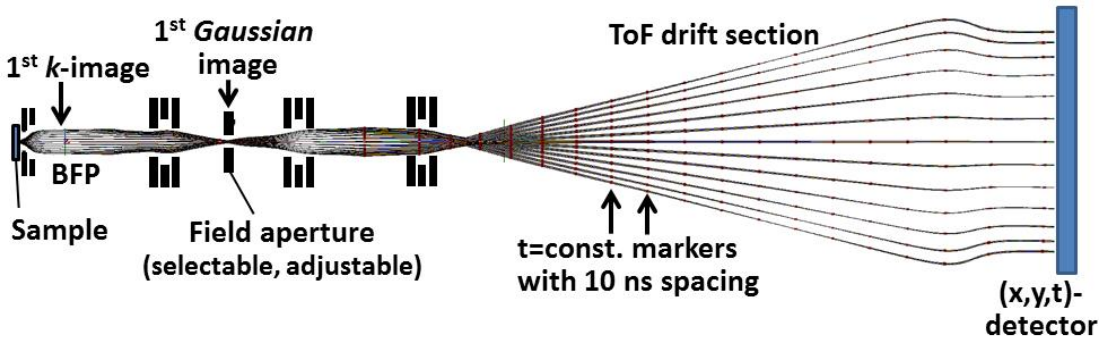

Figure 3. Cross section of the ToF ***k***-microscope with trajectories for 100 eV starting energy on the sample (lens elements schematic). In this case the drift energy is 30 eV, corresponding to an expected energy resolution of 30 meV.

A special property of the ToF ***k***-microscope is the small distortion of the isochronous surfaces. The dots at each trajectory denote time markers with 10 ns spacing, which are located on planes as visible until the end of the drift section. In other words, there is essentially no correlation between the transversal momentum and the kinetic energy. This is an outstanding feature of the present instrument, different

https://doi.org/10.1017/S1431927615013240 Published online by Cambridge University Press

from other spectroscopic ToF devices. There are two reasons for this: (i) the cathode lens is a strong immersion lens causing a virtual image of the source at twice the distance from the extractor electrode with an apparently much higher starting energy of 10-20 keV (depending on the extractor potential) and a much smaller cone of effective emission angles; (ii) the radial coordinate in Fig. 3 is 8× stretched, i.e. in an isogonic plot all rays run very close to the axis.

The principle of data acquisition is illustrated in Figure 4. All counting events in the E-$\boldsymbol{k}_{\parallel}$ paraboloid confined by the constant energy surface at the Fermi energy E_F and the photoemission horizon (condition $k_{\perp}$=0) are detected at fixed setting of the $\boldsymbol{k}$-microscope. The binding energy (with respect to E_F) is determined as in classical photoemission ($E_B = h\nu - E_{kin} - \Phi$; Φ for work function) utilizing the relation $E_{kin} \propto ToF^{-2}$. The software of the delay-line detector accumulates counting events in the ($\boldsymbol{k}_x$,$\boldsymbol{k}_y$,E_B)-voxels of the data matrix. For visualization, sections or 3D tomograms can be made in every plane.

For the first experiments a frequency-doubled Ti-sapphire laser was used for 2PPE excitation at 2hν = 5.8–6.6 eV. Mapping a complete data set with good statistics requires only few minutes of acquisition time. Figure 4b,c shows an example taken for the Mo(110) surface. Here, a "Dirac-like" state with linear dispersion in a large energy range arises in a spin-orbit induced partial band-gap region, for details, see [12]. A similar state of this kind was first observed on W(110) by Miyamoto et al. [13,14].

Under non-optimal conditions of the first experiments (the instrument went into operation in Jan. 2014), the energy- and $\boldsymbol{k}$–resolution were about 60 meV and 2×10^{-2} Å^{-1}, respectively. For the Ti-sapphire experiment in Figure 4b,c (energy interval 1.5 eV, diameter of observed $\boldsymbol{k}_{\parallel}$–disc 1.4 Å^{-1}), we arrive at a total number of 3,900 resolved $\boldsymbol{k}$-points x 25 energy intervals = 10^5 ($\boldsymbol{k}_x$,$\boldsymbol{k}_y$,E_B)-voxels acquired simultaneously. In the first experiment with Synchrotron radiation (hν = 35 eV) at BESSY (Berlin) the energy- and $\boldsymbol{k}_{\parallel}$–range was increased to 4 eV and diameter 3.4 Å^{-1}, respectively, increasing the number of voxels to 3×10^5 [12]. Under optimized conditions, more than 5,000 $\boldsymbol{k}$-points can be resolved with this kind of electron optics [3]. The ToF method is expected to reach an energy resolution in the range of <10 meV. This will drive the degree of parallelization towards the order of 10^6 voxels.

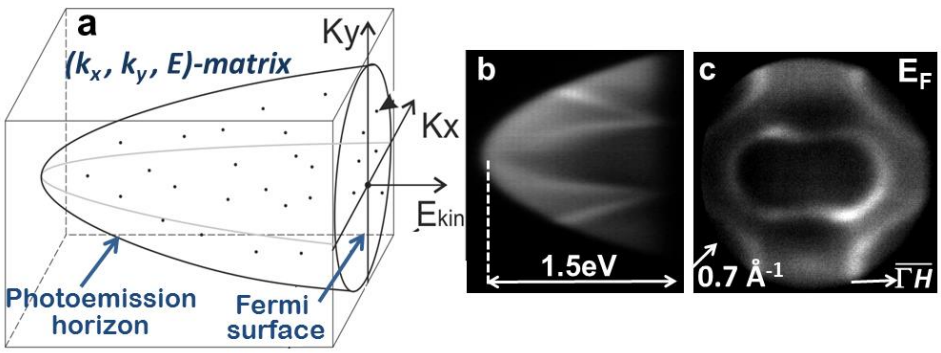

Figure 4. 3D data acquisition principle of a ToF $\boldsymbol{k}$-microscope. Schematic view of the ($\boldsymbol{k}_x$,$\boldsymbol{k}_y$,E_B) data matrix acquired simultaneously (a). The sections show the bands in an E-$\boldsymbol{k}_{\parallel}$ plane confined by the parabolic photoemission horizon and the Fermi energy (b) and the momentum disc at the Fermi surface (c) of Mo(110), taken with 2PPE excitation by 3.3 eV photons from a Ti-sapphire laser. (data from [12]).

https://doi.org/10.1017/S1431927615013240 Published online by Cambridge University Press

As test case for a material with high scientific interest we have chosen the topological insulator Bi_2Te_3, because detailed data with conventional high-resolution ARPES spectrometers exist [e.g. 15]. This material was cleaved in UHV in order to obtain a clean and well-defined surface. Figure 5 shows a collection of sections through several planes in the vicinity of the Dirac cone (V-shaped feature on top of the left figure). Note that Figure 5 shows the raw data without any treatment (like symmetrization). This 3D data matrix has been taken in a few minutes of total acquisition time.

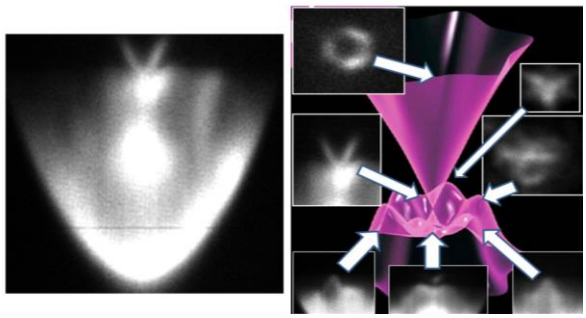

Figure 5. Result of a first measurement on a sample of the topological insulator Bi_2Te_3 (sample courtesy R. Claessen and M. Scholz, Univ. Wuerzburg, Germany). Many details of the Dirac state (topological surface state shown in $E_B(k_x,k_y)$ representation) are resolved in this run of only 5 minutes total acquisition time. The figure shows the raw data taken at room temperature.

Finally, we discuss the possibility of implementing an imaging spin filter into an instrument like the one shown in Figure 3. Although state-of-the-art spin detectors have reached good overall performance and ability for vectorial analysis [16], the basic concept of present spin polarimeters is not compatible for a use with parallel-imaging instruments. Recent developments towards multichannel spin detection in combination with a hemispherical analyzer [17] and with an emission electron microscope [6,3] exploit the fact that in low-energy electron diffraction $\boldsymbol{k}_{\parallel}$ is conserved, similar to an optical mirror, as illustrated in Figure 6a. With Ir(001) [18] and Ir(001)-Au(1x1) [19] spin-filter surfaces with high figure of merit and long lifetime in UHV have been found. For high-Z materials the diffraction process is highly spin selective, usable maxima of the spin asymmetry function reach 82%.

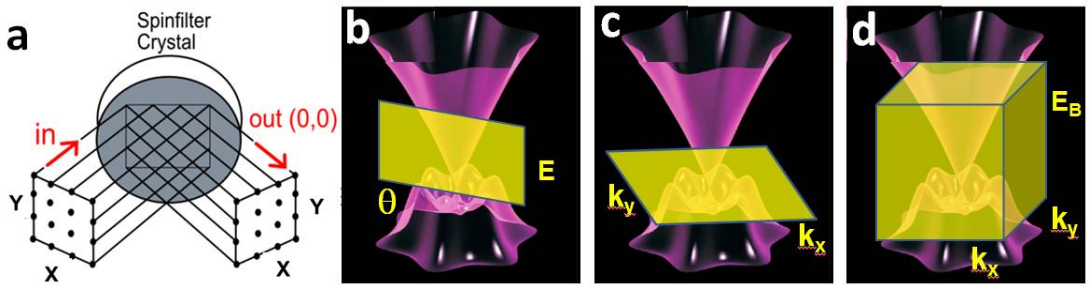

Figure 6. Basic scheme of parallel spin-polarization detection utilizing specular diffraction from a high-*Z* spinfilter crystal (a) and the application modes in combination with a hemispherical analyzer (b), with a ***k***-microscope with dispersive energy filter (c) and with a ***k***-microscope with time-of-flight detection (d). The 3D pattern in b, c and d shows a calculated topological surface state in $E_B(k_x,k_y)$ representation.

https://doi.org/10.1017/S1431927615013240 Published online by Cambridge University Press

Implementation of such a spinfilter in a hemispherical analyzer constitutes multichannel spin detection as demonstrated in [17] with about 10^3 (E,θ)-data points acquired simultaneously, schematized in Figure 6b. A hemispherical analyzer can detect a certain kinetic energy (E) and polar emission angle (θ) range in parallel. The high data acquisition speed made it possible to prove half metallicity in the Heusler compound Co_2MnSi [20], being hardly possible with a common single-channel spin detector due to the fast contamination of the reactive Heusler surface. Parallel acquisition of more data points has been achieved by integrating a spin-filtering electron mirror in an emission microscope with dispersive energy filter [6], in the present stage of development yielding > 10^4 (k_x,k_y) data points in parallel [3], sketched in Figure 6c. Sequential acquisition of $\boldsymbol{k}_{\parallel}$-distributions at many energies yields the complete spin-resolved valence band structure.

As an outlook, ToF **k**-microscopy with imaging spin filter will allow for parallel detection of the energy coordinate (via the time of flight) and thus adds the third dimension in parallel data acquisition, as depicted in Figure 6d. This new approach requires solving several problems like the energy-dependence of the spin asymmetry or the chromatic aberration of the electron-optical system. [21]

References:

[1] MZ Hasan and JE Moore, Annu. Rev. Cond. Matt. Phys. **2** (2011), p. 55.
[2] E Bauer, Rep. Prog. Phys. **57** (1994, p. 895.
[3] C Tusche *et al*, submitted for publication.
[4] A Winkelmann *et al*, Phys. Rev. B **86** (2012), 085427.
[5] A Winkelmann *et al*, N. J. Phys. **14** (2012), 0430009.
[6] C Tusche *et al*, Appl. Phys. Lett. **99** (2011), 032505.
[7] G Schönhense *et al*, Surf. Sci. **480** (2001), p. 180.
[8] A Oelsner *et al*, Rev. Sci. Instrum. **72** (2001), p. 3968.
[9] A Oelsner *et al*, J. Electron. Spectrosc. **178-179** (2010), p. 317.
[10] http://www. surface-concept.com.
[11] H Spiecker *et al*, Nucl. Instr. and Meth. A **406** (1998), p. 499.
[12] S Chernov *et al*, submitted for publication, S Chernov, PhD Thesis, in preparation.
[13] K Miyamoto *et al*, Phys. Rev. Lett. **108** (2012), 066808.
[14] K Miyamoto *et al*, Phys. Rev. B **86** (2012), 161411.
[15] S Souma *et al*, Phys. Rev. Lett. **106** (2011), 216803.
[16] F Meier *et al*, Phys. Rev. B **77** (2008), 165431.
[17] M Kolbe *et al*, Phys, Rev. Lett. **107** (2011), 207601.
[18] D Kutnyakhov *et al*, Ultramicrosc. **130** (2013), p. 63
[19] J Kirschner *et al*, Phys. Rev. B **88** (2013), 125419.
[20] M Jourdan *et al*, Nat. Commun. **5** (2014), p. 3974.
[21] The author would like to thank all people being involved in the developments discussed in this paper, in particular his coworkers and colleagues K. Medjanik, S. Chernov, D. Kutnyakhov, F. Schertz, D. Panzer, S. A. Nepijko and H. J. Elmers. Thanks are also due to the colleagues in Halle, C. Tusche, A. Krasyuk and J. Kirschner as well as to A. Oelsner (Surface Concept GmbH). Further thanks go to the staff of BESSY (in particular C. Schüssler) and to R. Claessen and M. Scholz (Univ. Wuerzburg) for providing the Bi2Te3 crystal. Financial support by DFG (Scho 341/9) and BMBF (05K12UM2, 05K12EF1 and 05K3UM2) and the center CINEMA, Mainz is gratefully acknowledged.